Review of Corrosion Kinetics and Thermodynamics of CO_2 and H_2S Corrosion Effects and Associated Prediction/Evaluation on Oil and Gas Pipeline System.

Obuka, Nnaemeka Sylvester P., Okoli Ndubuisi Celestine, Ikwu, Gracefield Reuben O., Chukwumuanya, Emmanuel Okechukwu

Abstract: In order to control the corrosion in pipelines, it is important to understand the underlying corrosion mechanisms and prediction of it's initiation and means of mitigation. This paper reviews the electrochemistry of corrosion, it's kinetics and thermodynamic nature, with respect to CO_2 and H_2S effects in propagating corrosion in oil and gas pipeline system. The phenomenon of polarization and it's importance in the mitigation of corrosion processes was highlighted in relation to it's mechanisms. Several principles and models used in predicting and evaluating corrosion kinetics were reviewed emphasizing their applicability in the oil and gas pipeline system. Scale formation on metal surface plays a prominent role in the rate of corrosion propagation making the process more complex, hence the mathematical models to extract the parameters which determine the effect of scale formation were appraised.

Keywords: Electrochemistry, Kinetics, Thermodynamic, Scale formation, Pipeline, Polarization, Corrosion

1 INTRODUCTION

The condition for a spontaneous reaction, changing the state of any material is that the reaction takes place with the release of energy. If such a thermodynamic driving force exists for a corrosion process, the next question is, at what rate or level of effects does the particular corrosion proceed or have? [1]. The presence of carbon(IV)oxide (CO_2), hydrogen sulphide (H_2S) and free water can cause severe corrosion problems in oil and gas pipelines. Internal corrosion in wells and pipelines is influenced by temperature, CO_2 and H_2S content, water chemistry, flow velocity, oil or water wetting and composition and surface condition of the steel [2]. Corrosion by carbon(IV)oxide with or without the presence of hydrogen sulphide is an important issue in the oil and gas industry. The severity of corrosion depends apart from the aforementioned factors also on pressure, pH, composition of the aqueous steam, partial pressures of CO_2 and H_2S and presence of non aqueous phases [3]. Corrosion of steel by CO_2 and CO_2/H_2S has been one of the major problems in the oil and gas industry since 1940. Recently, it has again come to the limelight, because of the technique of CO_2 injection for enhanced oil recovery and exploitation of deep natural gas reservoirs containing carbon(IV)oxide [4].

- *Obuka Nnaemeka Sylyester is currently pursuing doctor of philisophy degree program in Industrial/Production engineering department in Nnamdi Azikiwe University, Nigeria, E-mail: silvermeks7777@yahoo.com*
- *Okoli Ndubuisi Celestine; Ikwu Gracefield Reuben; and Chukwumuanya Emmanuel Okechukwu are currently pursuing the same degree program as the corresponding author in the same department and in the same University.*

The effect of corrosion was found to supersede a simple mass loss of metal, while galvanic cell formation due the presence of these gaseous ions in oil and gas installations constitutes the major agent of corrosion [5]. In the presence of CO_2 corrosion rate can be reduced substantially under conditions when corrosion product, iron(III)trioxocarbonate(V)[$FeCO_3$] can precipitate on the steel surface and form a dense and protective corrosion product film. This occurs more easily at high temperature or high pH in the water phase. When corrosion products are not deposited on the steel surface, very high corrosion rates of several millimeters per year can occur. When H_2S is present in addition to CO_2, iron sulphide (FeS) films are formed than $FeCO_3$. This protective film can be formed at lower temperature, since FeS precipitates much easier than $FeCO_3$. Localized corrosion with very high corrosion rates can occur when the corrosion product film does not give sufficient protection, and this is the most feared type of corrosion attack in oil and gas pipelines. The major concern with CO_2 corrosion in oil and gas industry is that CO_2 corrosion can cause failure on the equipment especially the main downhole tubing and transmission pipelines and thus disrupt the oil and gas production. Its chemical reactions include CO_2 dissolution and hydration to form carbonic acids as shown in (1) and (2);

$$CO_{2(g)} \rightarrow CO_{2(aq)} \quad (1)$$

$$CO_2 + H_2O \rightarrow H_2CO_3 \quad (2)$$

The trioxocarbonate (V) acid then dissociates into bicarbonate and carbonate in two steps as in (3) and (4)

$$H_2CO_2 \rightarrow H^+ + HCO_3^- \quad (3)$$

$$HCO_3^- \rightarrow H^+ + CO_3^{2-} \quad (4)$$

CO_2 corrosive action on iron is an electrochemical reaction with the overall reaction given as;

$$Fe + CO_2 + H_2O \rightarrow FeCO_3 + H_2 \quad (5)$$

Hence, CO_2 corrosion leads to the formation of a corrosion product, $FeCO_3$, which when precipitated could form a protective or non-protective scale depending on the environmental conditions of pH scale, temperature, etc. [6]. The internal corrosion of carbon steel in the presence of hydrogen sulphide represents a significant problem for both oil refineries and natural gas treatment facilities. The scale growth which is one of the factors governing the corrosion rate is dependent on the kinetics of surface scale formation. In an H_2S environment many types of iron sulphide may form such as amorphous ferrous sulphide, mackinawite, cubic ferrous sulphide, smythite, greigte, pyrrhotite, troilite and pyrite, among which mackinawite is considered to form first on the steel surface by a direct surface reaction [7]. The poorly known mechanism of H_2S corrosion makes it difficult to quantify the kinetics of iron dissolution in aqueous solutions containing H2S based on the formation of mackinawite film, as proposed by Sun et al, 2008, is shown in figure 1. The understanding of the effect of H_2S on CO_2 corrosion is still limited because of the nature of the interaction with carbon steel is complicated. Dissociation of dissolved H_2S is given in (6);

$$H_2S \xrightarrow{K_{H_2S}} H^+ + HS^- \qquad (6)$$

While the dissolution of HS- is given by equation (7);

$$HS^- \xrightarrow{K_{HS^-}} H^+ + S^{2-} \qquad (7)$$

Where $K_{H_2S} = \frac{[H^+/HS^-]}{H_2S}$ and $K_{HS^-} = \frac{[H^+/S^{2-}]}{HS^-}$

In a H_2S dominated system or CO_2/H_2S mixed system, the direct reduction of H_2S lowers the solution's pH as it acts as a weak acid and increases the corrosion rate by providing an extra cathodic reaction, similar to the action of trioxocarbonate(V)acid, as shown in (8), [9].

$$H_2S + e^- \rightarrow H + HS^- \qquad (8)$$

However, when H_2S is present in low concentration in a CO_2 dominated system, the iron sulphide (FeS) film interferes with the formation of the carbonate scale ($FeCO_2$). This is of interest because the iron sulphide film would seem to be more easily removed from the pipe wall than the iron carbonate scale [10]. Under turbulent conditions, removal of the protective scale will lead to an increased corrosion rate [11]. The kinetics of surface scale formation in the CO_2/H_2S system is complicated; depend on the competitive kinetics of the two scale formation mechanism, and also on the chemistry of the brine and the respective solubility of iron carbonate and iron sulphides [12]. Corrosion process can therefore take place if there is a thermodynamic force driving the process. The rate of corrosion can, however, vary within wide limits. In certain cases it can be large and cause serious damage to the material, and other cases can be small, of little practical importance. Therefore, it is imperative to study the mechanism of these kinetics and thermodynamics of corrosion vis-à-vis their effects on oil and gas pipeline system.

2 MATERIALS AND METHODS

2.1 Corrosion Kinetics and Electrochemistry

Thermodynamic principles can explain a corrosion situation in terms of the solubility of chemical species and reactions associated with corrosion processes. However, thermodynamic principles cannot be used to predict corrosion current or corrosion rate [13]. On an electrode (pipeline) immersed in an aqueous solution, both an oxidation and a reduction may occur. These proceed as an oxidation of metal atoms to ions and a reduction of metal atoms in accordance with the equation;

$$Me \rightleftharpoons Me^{n+} + ne^- \qquad (9)$$

An equilibrium potential (E_{eq}) is associated with each reaction. When a current is applied to the electrode surface the electrode potential charges and the electrode is said to be polarized. The difference between this resultant potential (E) and each electrode's reaction equilibrium potential (E_{eq}) is called polarization or overpotential (η) and it is modeled as;

$$\eta = E - E_{eq} \qquad (10)$$

The polarization can be anodic or cathodic, when the processes on the electrode are accelerated by moving the potential in the positive or negative direction respectively. There are there basic types of polarization, as expressed in (11);

$$\eta_{total} = \eta_{act} + \eta_{conc} + iR \qquad (11)$$

Where, η_{act} is the activation overpotential, η_{conc} is the concentration overpotential and iR is the ohmic drop. The expression relating the overpotential η, to the net current i, is the Butler-Volmer equation:

$$i = i_o \left\{ exp\left(\beta . \frac{nF}{RT} . \eta\right) - exp\left(-[1-\beta] . \frac{nF}{RT} . \eta\right) \right\} \qquad (12)$$

The first term in {} in Butler-Volmer describes the forward (metal dissolution, anodic) reaction, while the second term in {} describes the backward (metal deposition, cathodic) reaction [14]. In the Butler-Volmer equation R, is gas constant; T, is the absolute temperature; n, is the number of charges transferred (valency); F, is the Faraday constant; β, is the symmetry coefficient and i_0, is the exchange current. Activation polarization is a complex function describing the charge transfer kinetics of an electrochemical reaction. It is always present and the main polarization component at small polarization currents or voltages. Activation overpotential is usually the controlling factor during corrosion in strong acids since both η_{conc} and iR are relatively small. Concentration polarization is a function describing the mass transport limitations associated with electrochemical processes and it's dominant at larger polarization currents or voltages. It usually predominates when the concentration of the active species is low. The ohmic drop takes into account the electrolytic resistivity of an environment when the anodic and cathodic elements of a corrosion reaction are separated by this environment while still electrically coupled. The ohmic drop will become an extremely important factor when studying corrosion phenomena for which there is a clear separation of

the anodic and cathodic corrosion sites, e.g. crevice corrosion. It is also an important variable in the application of protective methods such as anodic and cathodic protections that force potential shift of protected structures by passing current into the environment [15]. Knowledge about the kind of polarization which is occurring can be very helpful in corrosion mitigation, since it allows an assessment of the determining characteristics of a corroding system. For example, if corrosion is controlled by concentration polarization, then any change that increases the diffusion rate of the active species (e.g. oxygen) will also increase the corrosion rate. In such a system, it would therefore be expected that agitating the liquid or stirring it would tend to increase the corrosion rate of the metal, as in case of a turbulent flow through the pipeline. However, if a corrosion reaction is activation controlled then stirring or increased agitation will have no effect on the corrosion rate.

2.2 Kinetics Data Graphics

In order to model a corrosion situation with mixed potential diagrams, the information concerning the following must be available; (1) activation overpotential for each corrosion process involved and (2) any additional information for process that could be affected by concentration overpotential. According to the mixed-potential theory underlying these diagrams, any electrochemical reaction can be algebraically divided into separate oxidation and reduction reactions with no net accumulation of electric charge. At this point the net measurable current is zero and the corroding metal is charged neutral.

2.2.1 Activation Overpotential Processes

In activation controlled corrosion processes (figure 2), reactions are depicted by straight lines on an E versus Log i plot, with positive Tafel slopes for anodic processes and negative Tafel slopes for cathodic processes. Figure 2 is polarization behavior of carbon steel in a deaerated solution maintained at 25°C with a pH of zero. The outline is the polarization plot and the dotted lines represent the anodic reaction of (13) and the cathodic reaction of (14) that depict the corrosion behavior of steel in these conditions.

$$Fe_{(s)} \rightarrow Fe^{2+} + 2e^{+} \quad (13)$$

$$2H^{+} + 2e^{+} \rightarrow H_{2(g)} \quad (14)$$

The sharp peak observed at -0.221V vs Standard Hydrogen Electrode (SHE) estimates the corrosion potential (E_{corr}), while the dotted lines from the point where the current crosses zero i.e. infinity on a log scale, find the intercept which indicates the cancellation between anodic and cathodic current. The current density of 67μA/cm^2 evaluated in this example corresponds to a penetration rate of 0.8mm/y. under the same condition but at a different pH of five (figure 3), the shift of the E_{corr} to a more negative value of -0.368V vs SHE is observed. The modeled projected lines provide a corrosion current of 4μA/cm^2 corresponding to a penetration of 0.5mm/y.

2.2.2 Concentration Overpotential Processes

In a concentration controlled process, one of the reactions is limited by the rate of transport of the reactant to the metallic surface being corroded. The system in this situation is at pH of five, 25°C and the environment is both aerated and stagnant (figure 4). A second cathodic reaction is made possible by oxygen reduction.

$$O_2 + 4H^{+} + 4e^{-} \rightarrow 2H_2O \quad (15)$$

The intercept where the opposing current are balanced occurs at an E_{corr} of -0.33V vs SHE, with a current density of 8.2μA/cm^2 to a penetration of 0.1mm/y. when the reduction of oxygen is enhanced through the agitation of the environment, the limiting current is increased by a tenfold factor to reach the value of 63μA/cm^2 a new situation emerges as depicted in figure 5. The marked positive shift of E_{corr} is now -0.224V vs SHE, and accompanied by an increase in current density of 63μA/cm^2 at a penetration rate of 0.8mm/y.

3 Corrosion Kinetics Principles, Models and Rates Calculation

There are three basic kinetics principles or laws that characterize the oxidation rates of pure metals; (a) parabolic rate law (b) logarithmic rate law and (c) linear rate law. These laws are modeled respectively as follows:

$$x^2 = K_p t + x_o \quad (16)$$

$$x = K_p \log(ct + b) \quad (17)$$

$$x = K_L t \quad (18)$$

The parabolic rate law makes the assumptions that the concentrations of diffusing species at the oxide-metal and oxide-gas interfaces are constant, and that the oxide layer has to be uniform, continuous and of the single phase type. This law is applicable to high temperature engineering problems. While the logarithmic and the linear rate laws are both empirical relationships. However, metals with linear oxidation kinetics at a certain temperature have a tendency to undergo the so-called catastrophic oxidation [16]. The analysis of para-linear kinetics behavior caused by a parabolic rate weight gain and a linear weight loss that occur at the same time can be carried out using the Tedmon equation:

$$\frac{d_x}{d_t} = \frac{k_p}{x} - k_v \quad (19)$$

In a situation where $K_v / K_p < 1$, equation (19) becomes;

$$x = K_v t + \left(K_v^2 t^2 + 2K_p t\right)^{1/2} \quad (20)$$

Where x, is the scale thickness; K_p, is the parabolic rate constant for scale growth; K_v, is the linear rate constant for loss of scale by volatilization, and t, is time. The kinetics model of (20), can be considered in terms of weight changes due to high vapor pressure at temperatures above 500°C, to become;

$$w = -K_v t + \left(K_v^2 t^2 + 2K_p t\right)^{1/2} \quad (21)$$

By metallography, the extent of metal loss and scale thickness can be determined through this model:

$$\frac{w}{A_o} = \frac{w_g}{A_o} - \frac{w_l}{A_o} \quad (22)$$

Where w, is the measured weight gain after time, t; w_g, is the total weight of the scale; w_l, is the total weight of metal lost from the specimen core; and A_o, is the original specimen area. Also using metallographic measurements, rate constants could be calculated for the growth of the scale assuming parabolic behavior and for metal loss assuming linear behavior, as can be expressed by (23) and (24).

$$\frac{w_g - w_s}{A_o} = \left(K_{pc} \times t\right)^{1/2} \quad (23)$$

$$\frac{w_v}{A_o} = -K_{ve} \times t \quad (24)$$

Where K_{pc}, is the empirical parabolic rate constant for the scale growth, and K_{ve}, is the empirical linear rate constant for metal loss by vaporization. The rate of corrosion can be large, causing serious damage to materials, some cases small, being as a result of inhibition of one or more of the electrode reactions. Extent of corrosion can be expressed in terms of; (i) change in weight of the metal, (ii) depth of the surface zone which has corroded away, (iii) number and quantity of pits formed, (iv) amount of corrosion products and (v) changes in the ultimate strength, yield strength or rupture strain of the metal. Equation (25) expresses corrosion rate in terms of mass loss, thus [17].

$$R_c = \frac{K(m_b - m_a)}{A(\Delta t)\rho} \quad (25)$$

Where R_c, is corrosion rate (mm/y); m_b, is mass before exposure (g); m_a, is mass after exposure (g); A, is exposed surface area (mm^2); Δt, is exposure time (hrs); ρ, is density (g/cm^3) and K, is constant for unit conversion. The rate of corrosion is also quantified through the relationship between the corrosion current density (i_{corr}) and metal dissolution (corrosion) rate, as in (26):

$$R_c = \frac{M}{nF_\rho} i_{corr} \quad (26)$$

Also the ratio M/n, is referred to as Equivalent Weight (EW) of individual element constituent of alloy, hence (26) can be expressed as;

$$R_c = K\frac{i_{corr}}{F_\rho}(EW) \quad (27)$$

Where M, is the atomic weight of the metal (g/mol), n, is the charge number (electron valency), F, is the Faraday's constant and EW for an alloy is given by the relation of (28):

$$EW = \frac{1}{\sum \frac{n_i F_i}{A_i}} \quad (28)$$

Where n_i, is valence of alloying element, i ; F_i, is mass fraction of alloying element, i ; and A_i, is atomic mass of element, i (g/mol),[18].

4 Modeling of Surface Scale Formation Effects on Corrosion Rates

Corrosion processes become significantly more complex in the presence of solid scales that may form on the metal surface. In general, it is necessary to consider; (i) the precipitation equilibria on the metal surface (ii) anodic dissolution processes that occur on the free surface of the metal (iii) dissolution kinetics of the solid scale (iv) cathodic processes on the free metal surface (v) cathodic processes on the scale surface, which are expected to be considerably slower than those on the free surface (vi) local concentrations of active ions close to the metal surface, which are influenced by adsorption and mass transfer and (vii) transport of ions through scale, which depends on the permeability of the solid precipitate. In principle, it is possible to develop a truly comprehensive model that takes into account all these phenomena [19], [20]. However, such a model would contain a large number of parameters that could not be unequivocally determined on the basis of the limited amount of electrochemical and exposure data that are available in literature. In order to derive a mathematical model that represents the effects of scale formation on corrosion rates. Anderko and Young, 2002, considered n separate species that may be formed on the surface of the corroding metal. The fraction of the surface occupied by ith species is dented by θ_1 and it's change with time is expressed as:

$$\left[\frac{\partial\theta_i}{\partial t}\right]_{E,a} = j_i\left[1 - \sum_{k=1}^{n}\theta_k\right] - C_i\theta_i \quad (29)$$

Where j_i,is the rate constant for the formation of the ith species on the free surface of the metal and l_i, is the rate constant for the dissolution of these species. In the limit of stationary state (i.e., for $t \to \infty$) θ_1 is given as;

$$\theta_i = \frac{j_i}{l_i\left[1 + \sum_{k=1}^{n}\frac{j_k}{l_k}\right]} \quad (30)$$

The averaged effect of surface scale can be represented by (31) with the assumption that the partial current densities i are modified by the presence of the scale, thus;

$$i' = i\left(l - \sum_{k=1}^{n}\theta_k\right) = \frac{i}{l + \sum_{k=1}^{n}\frac{j_k}{l_k}} \quad (31)$$

And j_k can be rewritten as

$$j_k = j_k^* N_X^a N_Y^b \cdots \quad (32)$$

Where N_X, N_Y, etc., are surface concentration of appropriate active solution species, X, Y, etc., and a, b, etc., are reaction orders, thus;

$$i' = \frac{i}{1 + \sum_{k=1}^{n}\frac{j_k^* N_X^a N_Y^b \cdots}{l_k}} = \frac{i}{1 + \sum_{k=1}^{n} q_k N_X^a N_Y^b \cdots} \quad (33)$$

Assuming the Langmuir absorption behavior, N_X can be represented as;

$$N_X = \frac{k_r a_r}{1 + \sum_r k_r a_r} \quad (34)$$

The parameter q_k in (33) is the ratio of the rate constant for the formation and dissolution of scales; and k_r, characterizes the adsorption of the aqueous species that are responsible for scale formation. However, aside the bulk activity of species, the effect of scale formation is determined by the parameters, q_k and k_r. In case of a $FeCO_3$ scale, the HCO_3^- ion can be assumed to be the active species that participates in the scale formation because it is much more abundant than CO_3^{2-} in the pH region of $FeCO_3$ precipitation, i.e.,

$$Fe + 2HCO_3^- = FeCO_3 + H_2CO_3 + 2e^- \quad (35)$$

Thus, N_{HCO_3} is substituted for the term $N_X^a N_Y^b$ in (33). Since N_{HCO_3} depends on the activity of HCO_3^- ions, it is a strong function of solution chemistry. For the $FeCO_3$ scale, the parameter q_k has been found to be temperature-dependent according to an Arrhenius-type expression, thus;

$$q(T) = q(T_{ref}) exp\left[-\frac{\Delta q}{R}\left(\frac{1}{T} - \frac{1}{T_{ref}}\right)\right] \quad (36)$$

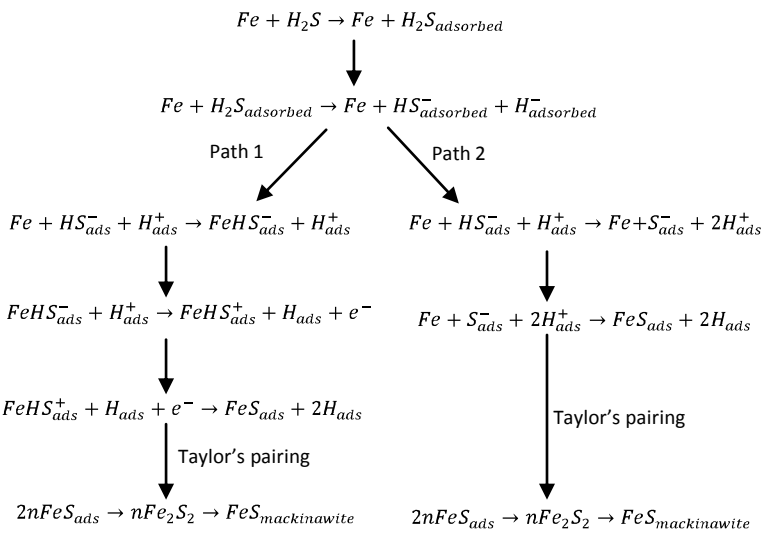

Figure 1: Mechanism of H_2S corrosion on Fe

Therefore, the parameters that are needed for the computation of the effect of $FeCO_3$ scaling are $q_{FeCO_3}(T_{ref})$, Δq_{FeCO_3}, and $K_{HCO_3^-}$.

5 Conclusion

Several prediction and mitigation models have been developed for CO_2 and H_2S corrosion of oil and gas pipeline. The models are correlated with different laboratory data and, in some cases, also with field data from oil companies. The models have very different approaches to accounting for oil wetting and the effect of protective corrosion films, which can give large difference in behavior between the models. It is not possible to declare one or two models as better than the others. But it is important to understand how the corrosion prediction models handle, particularly, the effects of these gases, oil wetting and protective corrosion films when the models are used for corrosion evaluation of wells and pipelines. There is inevitably a high degree of uncertainty in these predictions and no model should be believed to have more than $\pm 50\%$ accuracy for a wide range of conditions. However, the knowledge about te kind of overpotential or polarization occurring during corrosion processes is very helpful and important in corrosion mitigation, since it allows an assessment of the determining characteristics of a corroding system.

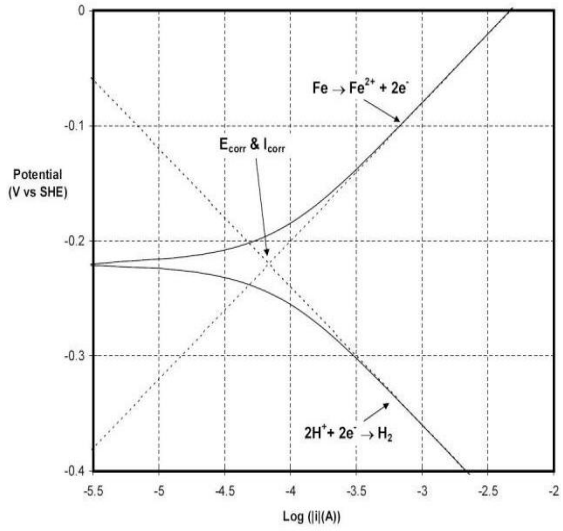

Figure 2: Polarization behavior or carbon steel in a deaerated solution maintained at 250C and a pH of zero

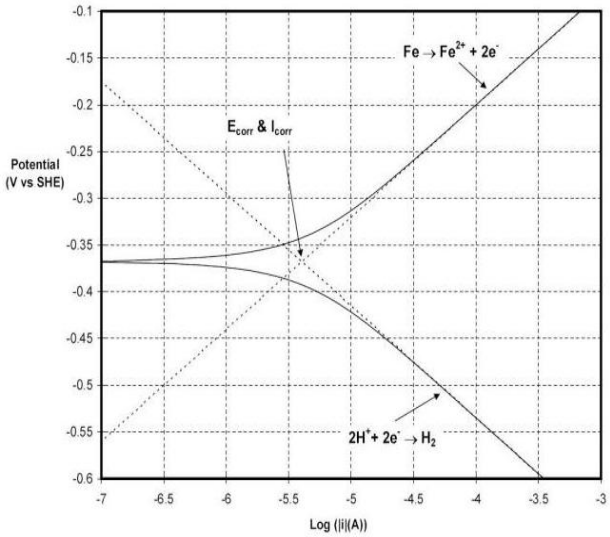

Figure 3: Polarization behavior or carbon steel in a deaerated solution maintained at 250C and a pH of five

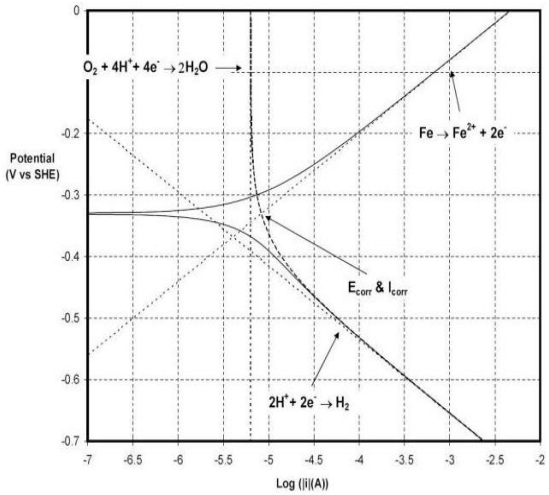

Figure 4: Polarization behavior or carbon steel in a stagnant aerated solution maintained at 250C and a pH of five

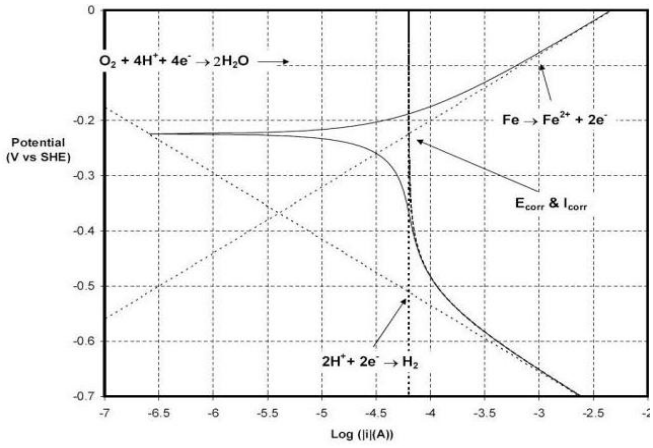

Figure 5: Polarization behavior or carbon steel in an agitated aerated solution maintained at 250C and a pH of five

REFERENCES

1. Enetanya, A.N. Corrosion problems in industrial mechanical systems. Joen Printing and Publishing Company, Ogui, Enugu, Nigeria, 2001; 10-12.
2. Nyborg, R. Controlling internal corrosion in oil and gas pipelines. Business Briefing Exploration and Production: Oil and Gas Review, 2005; Issue 2.
3. Anderko, A., and Young, R.D. Simulation of CO2/H2S corrosion using thermodynamic and electrochemical models. Corrosion/02, Paper No. 991, NACE International, Houston, Texas, 2002.
4. Zhao, G.X. et al. Formation characteristics of CO2 corrosion product layer of P110 steel investigated by SEM and electrochemical technique. Iron and Steel Research International, 2009; 16 (41): 89-94.
5. Obuka, S.P.N., and Ihueze, C.C. A review of corrosion and corrosion schemes for metal and composite oil and gas system: Management and development. Journal of Advanced Materials, 2011; 43 (2): 35-54.
6. Hunnik, E.W.J.V., Pots, B.F.M., and Hendriksen, E.L.J.A. The formation of protective FeCO3 corrosion product layers in CO2 corrosion. Corrosion/96, Paper No. 6, NACE International, Houston, Texas, 1996.
7. Sun, W., and Nesic, S. A mechanistic model of H2S corrosion of mild steel. Corrosion/07, Paper No. 07655, NACE International, Houston, Texas, 2007.
8. Sun , W., Marquez, A.I., and Bohe, G.G. Theoretical investigation of H_2S corrosion of mild steel. Institute of Corrosion and Multiphase Technology 2008.

9. Hausler, R.H., and Godard, H.P. Advances in CO2 corrosion. NACE International Publication, 1984: 1.
10. Koteeswaran, M. CO2 and H2S corrosion in oil pipelines. Masters Degree Thesis, Faculty of Mathematics and Natural Science, University of Stavanger, Norway, 2010.
11. Srinivan, S., and Kane, R.D. Prediction of corrosivity of CO2/H2S production environment. Prevention of Pipeline Corrosion Conference, Houston, Texas, 1995.
12. Sun, W., and Nesic, S. Kinetics of iron sulphide and mixed iron sulphide/carbonate scale precipitation in CO2/H2S corrosion. Corrosion/06, Paper No. 06644, NACE International, Houston, Texas, 2006.
13. Roberge, P.R. Corrosion basics: An introduction, 2nd edition. NACE Press Book, 2006: 56-70.
14. Lister, D.H. Corrosion for engineers. Lecture note, University of New Brunswick, Canada, 2005.
15. Roberge, P.R. Corrosion engineering: Principles and practice. McGraw-Hill Publishers, 2008: 85-106.
16. Boreman, D.J., Wimmer, B.O., and Lewis, K.G. Repair technologies for gas transmission pipelines. Pipeline and Gas Journal, New York, U.S.A. (2000).
17. Freeman, R.A., and Silverman, D.C. Error propagation in coupon immersion tests. Corrosion, 1992; 48 (6): 463.
18. Silverman, D.C. Practical corrosion prediction using electrochemical techniques. In Uhlog's Corrosion Handbook 2nd edition, R.W. Revie. Ed., John Wiley and Sons, 2000.
19. Ikeda, A., Ueda, M., and Mukai, S. Advances in CO2 corrosion. In R.H. Hausler and H.P. Godard, eds., Corrosion NACE International, Hoiston, Texas, 1984; 1: 39-51.
20. Sridhar, N., Dunn, D.S., Anderko, A., and Lencka, M.M. Final Report PR – 15 – 9712, Pipeline Research Committee International, Arlington, Virginia, 1984..